

## Semiclassical and quantum mechanical analysis of the excitation function for the $^{130}\text{Te}(p,n)^{130}\text{I}$ reaction

M. M. Musthafa, B. P. Singh, M. G. V. Sankaracharyulu, H. D. Bhardwaj,\* and R. Prasad  
*Department of Physics, Aligarh Muslim University, Aligarh (U.P.) 202 002, India*

(Received 19 December 1994)

We report excitation function for the reaction  $^{130}\text{Te}(p,n)^{130}\text{I}$  in the energy range  $\approx 4\text{--}18$  MeV. The measurements were done employing stacked foil activation technique and enriched isotope. To the best of our knowledge this excitation function has been reported for the first time. The theoretical analysis of the excitation function has been done employing both the semiclassical as well as quantum mechanical descriptions of the preequilibrium emission. In general, theoretical calculations agree well with the experimental data.

PACS number(s): 25.40.Kv, 27.60.+j

### I. INTRODUCTION

Preequilibrium (PE) emission, as a reaction mechanism at moderate excitation energies, has attracted considerable attention from both the experimental as well as the theoretical viewpoints [1]. Initially, semiclassical models [2–6] were successfully used to describe the experimental data on PE emission. Recently, however, the stress has been laid on the systematic study of trends with a view to finding a consistent set of input parameters that can describe the large amount of experimental data. Lately, totally quantum mechanical (QM) theories for PE emission have also been developed and have been used to analyze mostly the data on nucleon-induced reactions [7–11].

In the present work the excitation function for the reaction  $^{130}\text{Te}(p,n)^{130}\text{I}$  has been measured using the stacked foil activation technique. The analysis has been performed within the framework of both the semiclassical and QM models. The computer codes ALICE/LIVERMORE-82 [12] and ACT [13] have been used for the semiclassical treatment while the code EXIFON [14] has been employed for the QM calculations involving the multistep compound (MSC) and the multistep direct (MSD) formulations [7]. The details of the measurements are presented in Sec. II and the analysis of the data is discussed in Sec. III.

### II. EXPERIMENTAL DETAILS

In the present measurements the stacked foil activation technique [15] has been employed. An enriched isotope (61%) of tellurium (mass number=130) was used for preparing the samples, which were made by vacuum evaporation, of  $1.1\text{ mg/cm}^2$  thickness on aluminum backing of  $6.75\text{ mg/cm}^2$ . The square pieces of targets of size  $1.2\times 1.2\text{ cm}^2$  were used as samples in the stack. Each target was mounted individually on a conducting metal frame for heat dissipation. A stack for irradiation was made by taking seven targets with Al foils of suitable thickness as degraders, in between,

to have the desired energy at each target. The stack was irradiated by an unresolved diffused proton beam with an energy uncertainty of 0.5 MeV at the Variable Energy Cyclotron Centre (VECC), Calcutta, India. A tantalum collimator was used just before the sample stack to restrict the size of the beam to 8 mm diameter. The incident energies on the first and last foils were  $\approx 18$  and  $\approx 4.87$  MeV, respectively. The charge accumulated in the Faraday cup during the irradiation was measured using an ORTEC current integrator device. Further details of the experiment and the measurements are described elsewhere [16].

The  $\gamma$  counting of the irradiated samples was carried out using conventional Ge(Li)  $\gamma$ -ray spectroscopy. The detector was calibrated using various standard  $\gamma$  sources including a  $^{152}\text{Eu}$  source of known strength which was also used for determining the geometry-dependent detector efficiency for  $\gamma$  rays of different energies and at different source-detector distances. A typical efficiency curve at a source-detector distance of 6.4 cm is shown in Fig. 1. The  $\gamma$  rays of energies 418.0, 536.1, 668.56, 739.48, and 1157.49 keV emitted by  $^{130}\text{I}$  produced in the reaction  $^{130}\text{Te}(p,n)$  were identified. In

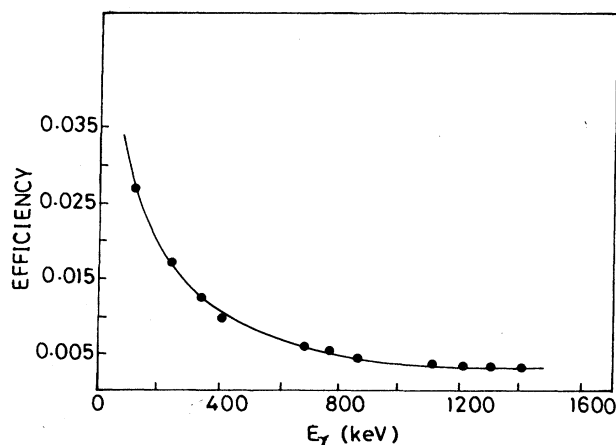


FIG. 1. Geometry-dependent efficiency of Ge(Li) detector at a source detector distance of 6.4 cm.

\*Present address: Department of Physics, D. S. N. College, Unnao (U.P.), India.

TABLE I. Measured and literature values of the intensities of  $\gamma$  rays emitted by  $^{130}\text{I}$ .

$\gamma$ -ray energy (keV)	Literature branching ratio (%) <sup>a</sup>	Measured values of		
		branching ratio (%) <sup>b</sup>	statistical errors of counting	overall errors
418.00	$34.2 \pm 0.1$	33.02	$\pm 0.08$	$\pm 2.72$
536.10	$99.0 \pm 0.5$	99.00	$\pm 0.20$	$\pm 8.12$
668.56	$96.1 \pm 0.6$	91.19	$\pm 0.20$	$\pm 7.50$
739.48	$82.3 \pm 0.7$	78.24	$\pm 0.19$	$\pm 6.45$
1157.49	$11.3 \pm 0.1$	9.21	$\pm 0.06$	$\pm 0.75$

<sup>a</sup>From Ref. [17].<sup>b</sup>Relative to 536.1 keV  $\gamma$  ray.

order to check the calibration of the detecting system, the energies and branching ratios for these  $\gamma$  rays were measured and are listed in Table I. Literature values [17] of the branching ratio for the same are also shown in this table. The errors in the literature data are only the statistical error of  $\gamma$  counting. The branching ratios were measured relative to the  $\gamma$  ray of 536.1 keV and may contain errors due to the following factors. (i) The statistical errors of counting which are tabulated in column 4 of Table I. (ii) Uncertainties in the absolute calibration of the geometry-dependent efficiency of the  $\gamma$ -ray detector. Since for the standard  $^{152}\text{Eu}$  point source, the counts were accumulated for a relatively larger time ( $\approx 3000$  sec), the uncertainty in the measured  $\gamma$  intensity of the standard source was negligible. The uncertainty due to the fitting of the measured efficiency by a power law graph was found to be  $<4\%$ . Uncertainties may also come up in the efficiency on account of the solid-angle effect since the irradiated samples were not point sources, but instead had a diameter of 8 mm. A detailed analysis of the solid-angle effect is given in Ref. [18]. Using this formulation the errors in the efficiency due to the solid-angle effect were estimated to be  $<4\%$ . Thus the overall errors in the measured branching ratio are  $\approx 8\%$  and are given in column 5 of Table I. From Table I, it may be seen that there is a reasonable agreement between the measured and the literature values [19–21] of the branching ratios for all the  $\gamma$  rays except for the 1157.49 keV  $\gamma$  ray for which we could not assign any reason.

The experimentally measured intensities of these  $\gamma$  rays have been used for calculating the cross sections according to the formula mentioned in Ref. [16]. The measured cross sections for the reaction  $^{130}\text{Te}(p, n)^{130}\text{I}$  at different incident proton energies ( $E_p$ ) are given in Table II. The first column in this table lists the incident energy on the foil while the second column lists the corresponding measured cross-section values. The errors in the energy in the first column represent the energy spread in half of the sample thickness along with the inherent energy uncertainty in the proton beam energy. The measured cross-section values at each energy reported in Table II in column 2 are the weighted averages of the cross sections calculated from the measured intensities of  $\gamma$  rays of different energies emitted by the residual nucleus  $^{130}\text{I}$ . In this table, column 3 contains the statistical error of counting only. However, in column 4 the overall errors are given which may be due to the following factors. (i) The statistical error of  $\gamma$  counting. (ii) The uncertainty in the determination of the number of target nuclei in the sample due to inaccurate determination of the sample

thickness and nonuniform deposition of the target material. To estimate the uncertainty in the number of target nuclei and to check the thickness and uniformity of the samples, pieces of different dimensions of the sample foils were weighed on an electronic microbalance and the thickness of each piece was calculated. In this way the errors in the estimation of the number of target nuclei were analyzed and are estimated to be  $<1\%$ . (iii) During the irradiation the beam current often fluctuates, which results in variation of the incident flux. Care was taken to keep the beam current fluctuations  $<10\%$ . In some typical irradiation runs the duration ( $>1$  min) and the amount of change in the beam current were noted during the irradiation and the flux was individually calculated for each duration of fluctuation. It is expected that the beam flux fluctuation may introduce errors of  $<3\%$ . (iv) The measured detector efficiency of the  $\gamma$  spectrometer may be inaccurate on account of the statistical errors in the counting of the standard source and the nonreproduction of identical geometry for the standard source and the sample. As already mentioned, the statistical errors in the counting of the standard source were minimized by accumulating a large number of counts for a comparatively larger time ( $\approx 3000$  sec). The uncertainties in the efficiency of the detector are estimated to be  $<8\%$ . (v) Beam intensity loss may occur as the beam traverses the thickness of the stack material. In the present experiment the total stack thickness reduces the incident proton energy from  $\approx 18$  to  $\approx 5$  MeV. The error in the measured cross section due to the maximum beam intensity loss at the end of the stack was estimated to be  $<1.5\%$ . (vi) The product nuclei recoiling out of the thin target may introduce errors in the measured cross sections. In the present measurements the targets were oriented perpendicular to the

TABLE II. Measured cross sections for  $^{130}\text{Te}(p, n)^{130}\text{I}$  reaction at different incident energies.

Incident proton energy $E_p$ (MeV)	Cross section (mb)	Statistical error of counting (mb)	Overall errors (mb)
$4.87 \pm 0.54$	8.76	$\pm 0.09$	$\pm 1.25$
$7.46 \pm 0.53$	282.34	$\pm 5.02$	$\pm 41.86$
$9.65 \pm 0.53$	262.51	$\pm 4.37$	$\pm 38.40$
$11.90 \pm 0.52$	132.15	$\pm 2.22$	$\pm 16.78$
$13.98 \pm 0.52$	94.85	$\pm 1.80$	$\pm 13.58$
$16.04 \pm 0.52$	77.91	$\pm 3.85$	$\pm 12.21$
$17.99 \pm 0.51$	100.24	$\pm 0.65$	$\pm 12.66$

beam with sample deposition facing the beam. This avoided the loss of recoiling nuclei which were stopped in the relatively thick ( $6.75 \text{ mg/cm}^2$ ) Al backing and were counted along with the sample. In this way the error due to recoiling nuclei has been eliminated. (vii) Errors may be introduced due to dead time, particularly for cases where the intensity of the induced activities in the sample was large. In such cases the sample-detector distance was suitably adjusted to minimize the dead time which was kept  $<10\%$  and corrections for which were applied in counting rates. The total error due to all these factors is expected to be  $<15\%$  of the measured cross-section values.

### III. ANALYSIS OF THE DATA

The analysis of the excitation functions has generally been carried out using the semiclassical theories [2–6]. However, in recent years the QM theories have also been applied extensively for nucleon-induced reactions [7–11]. In the present work we have analyzed the measured excitation function for the reaction  $^{130}\text{Te}(p,n)^{130}\text{I}$  using both the semiclassical as well as QM theories with the so-called global set of parameters. These parameters for the semiclassical approach were obtained from our earlier analysis of neutron and  $\alpha$ -induced reactions [13,16,22,23]. The computer codes ALICE/LIVERMORE-82 [12] and ACT [13] have been used for the semiclassical analysis, while the code EXIFON [14] has been used for the QM description of the data. Brief details of these codes and the parameters are summarized in the following sections.

#### A. Analysis with code ALICE/LIVERMORE-82

In the code ALICE/LIVERMORE-82 the compound nucleus (CN) calculations are performed using the Weisskopf-Ewing model [24] and the PE component is simulated employing the hybrid/geometry-dependent hybrid model [25]. The hybrid model is based on a combination of the exciton model [4] and the Harp-Miller-Berne model [3]. In the geometry-dependent hybrid model a decomposition is made according to incoming angular momentum in order to account for the effects of the nuclear density distribution, leading to increased emission of high energy particles. The binding energies are calculated using the Myer-Swiatecki/Lysekil mass formula [26] and the pairing energy  $\delta$  is calculated from the backshifted Fermi gas model [27]. The optical model parameters of Becchetti and Greenlees [28] are used for optical model (OM) calculations of the transmission coefficients. The intranuclear transition rates which determine the evolution of intermediate states may be adjusted in this code by varying the parameter COST, the mean free path multiplier. Values from 1 to 10 are suggested by Blann [5] for this adjustable parameter COST. Theoretically calculated excitation functions with the code ALICE using different values of the mean free path multiplier COST are shown in Fig. 2. In our earlier analyses of  $\alpha$ -induced reactions a value of COST = 3 has given satisfactory reproduction of the experimental data [22]. However, in the present calculations the excitation function calculated with COST = 3 underestimates the measured excitation function in the tail portion as shown in Fig. 2. As can be seen from this figure, COST = 9 gives a satisfactory reproduction of the measured data. The level density

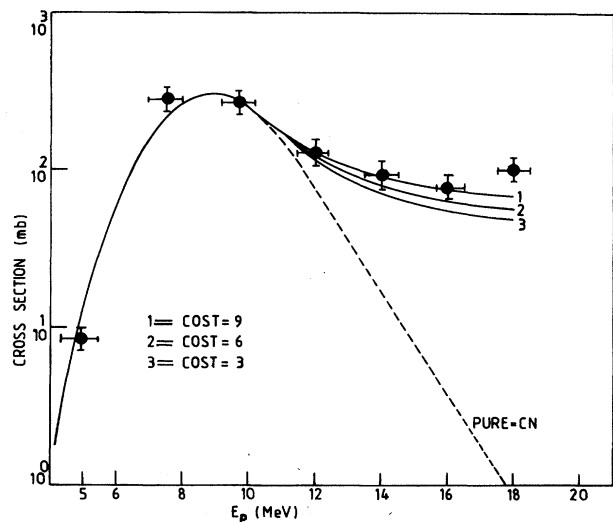


FIG. 2. Excitation functions calculated using the code ALICE. Solid curves show the calculations done using different values of the parameter COST. The dotted curve shows the pure CN component. ● shows the experimental data.

parameter  $a$  in this code is calculated from the expression  $a = A/K$ , where  $A$  is the atomic mass number of the compound system and  $K$  is a constant which can be varied to match the excitation functions. In the present calculations the value of  $K$  equal to 10 is kept. The same value of  $K$  was used in our earlier analyses of  $\alpha$ -induced reactions [22]. The initial configuration of the compound system, i.e., the initial exciton number, needed in these calculations is taken equal to 3 with two particles and one hole. It may be assumed that the first interaction of the proton with the target nucleus may give rise to the excitation of one particle above the Fermi energy leaving behind a hole in the excited state resulting in the two-particle and one-hole state.

#### B. Analysis with code ACT

In computer code ACT [13], the CN calculations are performed using the Hauser-Feshbach (HF) [29] model while the PE emission is simulated using the exciton model [4] of Griffin. In the HF formalism the angular momentum effects are explicitly considered at each step of deexcitation. The transmission coefficients needed in these calculations are generated using the optical model code TLK [13] which uses the OM potentials of Blann and Vonach [30]. The level density which determines the shape of both the equilibrium and preequilibrium components is an important parameter in these calculations. The level density parameter  $a$  and the fictive ground state energy  $\Delta$  are taken consistently from the tables of Dilg *et al.* [27]. The effective moment of inertia  $\Theta_{\text{eff}}$  is taken equal to the rigid-body value. The particle separation energies needed in the calculation are taken from the table of Wapstra and Gove [31].

The initial particle hole configuration  $n_0$  is also needed in these calculations. Here,  $n_0 = 3$  ( $n_p = 2$  and  $n_h = 1$ ) is taken, similar to the one taken in the code ALICE. In the exciton

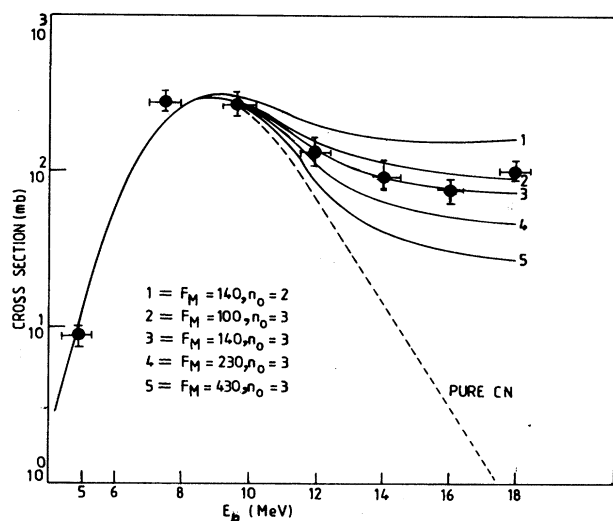


FIG. 3. Excitation functions calculated using the code ACT. Solid curves are for different values of  $F_M$  and  $n_0$ . The dotted curve shows the pure CN component. ● shows the experimental data.

model the intranuclear transition rates depend directly on the average of the square of the matrix element for two-body residual interactions  $|\bar{M}|^2$ . Its value is generally computed from the expression  $|\bar{M}|^2 = F_M A^{-3} U^{-1}$ , where  $A$  and  $U$  are the mass number and the excitation energy of the compound system, respectively, and  $F_M$  is generally treated as an adjustable parameter to match the measured and calculated excitation functions.  $F_M$  values ranging from 95 to 7000 MeV<sup>3</sup> have been proposed in the literature [10]. Excitation functions calculated with different values of  $F_M$  and  $n_0$  are shown in Fig. 3. In some of our earlier analyses of  $(n, p)$  and  $(\alpha, xn)$  reactions [13,16,22,23], a value of  $F_M = 430$  MeV<sup>3</sup> was found to give satisfactory reproduction of the experimental excitation functions. However, in the present case, the value of  $F_M = 140$  MeV<sup>3</sup> and  $n_0 = 3$  reproduces the measured excitation function satisfactorily in both the peak as well as the tail portions for this reaction. The dotted line in Fig. 3 shows the calculations for the CN component alone. In the exciton model it is assumed that the PE cross section is distributed among the levels with different spins and parity in the same proportion as the equilibrium contribution. This limitation may have important consequences for isomeric cross sections, but not for the total cross sections as presented in this paper.

### C. Analysis with code EXIFON

The code EXIFON [14] is based on an analytical model for statistical multistep direct and multistep compound reactions (SMD/SMC model) [7]. It predicts the activation cross section including the equilibrium and preequilibrium as well as the direct (collective and noncollective) processes within a pure statistical multistep reaction model. This approach is based on many body theory (Green's function formalism) [32,33] and random matrix physics [34,35]. The code EXIFON predicts the cross sections from a standard set of parameters [14]. The initial exciton number in this code is taken equal to 3 for nucleon-induced reactions, similar to the one taken in

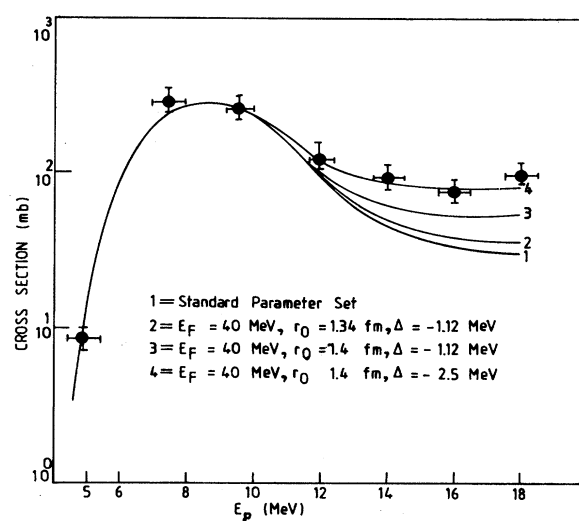


FIG. 4. Excitation functions calculated using the code EXIFON for different set of parameters. ● shows the experimental data.

semiclassical calculations. The calculation with the code EXIFON takes into account the pairing correction, Pauli blocking, shell structure, and the Coulomb effects. Figure 4 shows the excitation functions calculated using the code EXIFON with different sets of parameters. In this figure, curve 1 shows the excitation function calculated using the code EXIFON with a standard set of parameters. As can be observed from this figure, the calculation using the standard set of parameters underestimates the experimental data, particularly in the tail portion. In order to match the experimental data the values of some of the parameters have been changed from that of the standard set. The value of the pairing correction term  $\Delta$  has been changed from  $-1.12$  to  $-2.5$  which is in agreement with the value used by Kalbach-Cline, Huizenga, and Vonach [36] and Coryell [37]. The Fermi energy  $E_F$  is related to the single-particle state density  $g$  and through it to the level density parameter  $a$ . For  $E_F = 40$  MeV, using the formulation of Kalbach [38–41], Oblozinsky [42], and Avrigeanu *et al.* [43,44] one gets the value of  $a = 16$  for <sup>130</sup>Te and <sup>130</sup>I with radius parameter  $r_0 = 1.4$  fm. These values of  $E_F$  ( $= 40$  MeV) and  $r_0$  ( $= 1.4$  fm) are used in the present calculations with a residual interaction of 32 MeV.

From the above analyses it may be concluded that both the semiclassical as well as the QM codes, each with suitable choice of parameters, reproduce the experimental excitation function. As such there is no specific advantage in using the QM code over the semiclassical one. This is important since the QM calculations for complex particles in the incident channel are more intricate as mentioned by Kalka, Qaim, and Molla [45].

### ACKNOWLEDGMENTS

The authors thank the Chairman, Department of Physics, for providing the necessary facilities. Thanks are also due to Dr. S. N. Chintalapudi and the VECC personnel for all their help during the experiment over there. One of the authors (M.M.M.) acknowledges financial assistance from the UGC.

- [1] E. Gadioli and P. E. Hodgson, *Pre-equilibrium Nuclear Reactions* (Clarendon, Oxford, 1992).
- [2] R. Serber, Phys. Rev. **72**, 1114 (1947).
- [3] G. D. Harp, J. M. Miller, and B. J. Berne, Phys. Rev. **165**, 1166 (1968).
- [4] J. J. Griffin, Phys. Rev. Lett. **17**, 478 (1966).
- [5] M. Blann, Phys. Rev. Lett. **27**, 337 (1971).
- [6] J. Ernst, W. Friedland, and H. Stockhorst, Z. Phys. A **328**, 333 (1987).
- [7] H. Feshbach, A. K. Kerman, and S. Koonin, Ann. Phys. (N.Y.) **125**, 429 (1980).
- [8] T. Tamura and T. Udagawa, Phys. Lett. **78B**, 189 (1978).
- [9] T. Udagawa, K. S. Low, and T. Tamura, Phys. Rev. C **28**, 1033 (1983).
- [10] K. K. Gudima, S. G. Mashnik, and V. D. Taneev, Nucl. Phys. **A401**, 329 (1983).
- [11] R. Bonetti, M. B. Chadwick, P. E. Hodgson, B. V. Carlson, and M. S. Hussein, Phys. Rep. **202**, 171 (1991).
- [12] M. Blann and J. Bisplinghoff, Lawrence Livermore National Laboratory Report No. CA 94550, 1982.
- [13] H. D. Bhardwaj, Ph.D. thesis, Aligarh Muslim University, Aligarh, India, 1985.
- [14] H. Kalka, EXIFON-A statistical multistep reaction code, NEA Data Bank, Saclay, France, 1991.
- [15] E. V. Sayre, Annu. Rev. Nucl. Sci. **13**, 145 (1963).
- [16] B. P. Singh, M. G. V. Sankaracharyulu, M. Afzal Ansari, H. D. Bhardwaj, and R. Prasad, Phys. Rev. C **47**, 2055 (1993).
- [17] C. M. Lederer and V. S. Shirley, *Table of Isotopes* (Wiley, New York, 1978).
- [18] R. P. Gardner and K. Verghese, Nucl. Instrum. Methods **93**, 163 (1971).
- [19] E. Brown and R. B. Firestone, *Table of Radioactive Isotopes* (Wiley, New York, 1986).
- [20] P. K. Hopke, A. G. Jones, W. B. Walters, A. Prindle, and R. A. Meyer, Phys. Rev. C **8**, 745 (1973).
- [21] T. E. Fessler, G. M. Julian, and S. Jha, Phys. Rev. **174**, 1472 (1968).
- [22] B. P. Singh, Ph.D. thesis, Aligarh Muslim University, Aligarh, India, 1992.
- [23] J. P. Gupta, H. D. Bhardwaj, and R. Prasad, Pramana J. Phys. **24**, 639 (1985).
- [24] V. F. Weisskopf and D. H. Ewing, Phys. Rev. **57**, 472 (1940).
- [25] M. Blann, Phys. Rev. Lett. **28**, 757 (1972).
- [26] W. D. Myers and W. J. Swiatecki, Ark. Fys. **36**, 343 (1967).
- [27] W. Dilg, W. Schantl, H. K. Vonach, and M. Uhl, Nucl. Phys. **A217**, 269 (1973).
- [28] F. D. Becchetti and G. W. Greenlees, Phys. Rev. **182**, 1190 (1969).
- [29] W. Hauser and H. Feshbach, Phys. Rev. **87**, 366 (1952).
- [30] M. Blann and H. K. Vonach, Phys. Rev. C **28**, 1475 (1983).
- [31] A. H. Wapstra and N. B. Gove, Nucl. Data Tables **9**, 357 (1971).
- [32] P. Ring and P. Schuck, *The Nuclear Many-body Problems* (Springer-Verlag, New York, 1980).
- [33] A. B. Migdal, *Theory of Finite Fermi Systems and Applications to Nuclei* (Wiley Interscience, New York, 1970).
- [34] D. Agassi, H. A. Weidenmuller, and G. Mantzouranis, Phys. Rep. **22**, 145 (1975).
- [35] T. A. Broady, J. Flores, J. B. French, P. A. Mello, A. Pandey, and S. M. Wong, Rev. Mod. Phys. **53**, 385 (1981).
- [36] C. Kalbach-Cline, J. R. Huizenga, and H. K. Vonach, Nucl. Phys. **A222**, 405 (1974).
- [37] C. D. Coryell, Annu. Rev. Nucl. Sci. **2**, 331 (1953).
- [38] C. Kalbach, Nucl. Phys. **A172**, 255 (1971).
- [39] C. Kalbach, Z. Phys. A **283**, 401 (1977).
- [40] C. Kalbach, Z. Phys. A **287**, 319 (1978).
- [41] C. Kalbach, Z. Phys. A **332**, 157 (1989).
- [42] P. Oblozinsky, Phys. Rev. C **40**, 1591 (1989).
- [43] M. Avrigeanu and V. Avrigeanu, J. Phys. G **20**, 613 (1994).
- [44] M. Avrigeanu, M. Ivascu, and V. Avrigeanu, Z. Phys. A **335**, 299 (1990).
- [45] H. Kalka, S. M. Qaim, and N. I. Molla, Phys. Rev. C **45**, 1619 (1989).